Desalination and Water Treatment
www.deswater.com

doi: 10.5004/dwt.2017.20124

65 (2017) 98–108
February

Synthesis, application, and evaluation of palygorskite porous ceramsite as filter media in biological aerated filters

Teng Bao[a,b], Tianhu Chen[a,*], Marie-Luise Wille[c], Juan Tan[a], Dan Zhu[a], Dong Chen[a]

[a]*Laboratory for Nanominerals and Environmental Material, School of Resource and Environmental Engineering, Hefei University of Technology, China, emails: tengbao1222@sina.com (T. Bao), chentianhu@hfut.edu.cn (T. Chen), 917232085@qq.com (J. Tan), 928952924@qq.com (D. Zhu), cdxman@hfut.edu.cn (D. Chen)*
[b]*School of Chemistry, Physics and Mechanical Engineering, Science and Engineering Faculty, Queensland University of Technology, Australia*
[c]*Institute of Health & Biomedical Innovation, Queensland University of Technology, Brisbane, Australia, email: m.wille@qut.edu.au*

Received 20 February 2016; Accepted 1 August 2016

ABSTRACT

This study investigated a palygorskite porous ceramsite (PC) and commercially available ceramsite (CAC) as filter media in biological aerated filters (BAFs) for city wastewater treatment. We studied the difference between the two materials in terms of the removal of ammonia nitrogen (NH_3–N), total nitrogen (TN), total organic carbon (TOC), and phosphorus at a hydraulic retention time of 7 h and air-to-water ratios (A/W) of 1:1, 3:1, and 6:1. Results showed that PC-BAF was more efficient than CAC-BAF in removing the above-mentioned substances. For example, at the A/W of 3:1, the PO_4^{3-} removal was 77.71% with PC compared with 33.97% with CAC. Furthermore, TN removal was 45.70% with PC and 15.64% with CAC. The properties of PC were also analyzed through scanning electron microscopy, thermogravimetry, micro-computed tomography, and porosimetry. Given its well-developed porous structures, PC can promote the growth of microbial communities, improve the permeable capacity of microbial biofilm layers, and increase the removal efficiency of pollutants. Morphological analysis of the microbial biofilm also revealed that several microorganisms were successfully loaded on the surface of PC. These findings were further evaluated through polymerase chain reaction–denaturing gradient gel electrophoresis and sequence analysis of 16S rRNA gene fragments. *Flavobacterium* sp., *Sphaerotillus* sp., and *Nitrospira* sp. were primarily detected in PC-BAF. These microorganisms promote simultaneous nitrification and denitrification. Therefore, PC could be potentially used as a novel filter medium in BAFs to remove nitrogen and phosphorus simultaneously.

Keywords: Palygorskite; Porous ceramsite; Micro-computed tomography; Simultaneous removal of nitrogen and phosphorus; Microbial biofilm

1. Introduction

With rapid agricultural development, the treatment, reclamation, and utilization of agricultural wastes, which are essential for environmental maintenance and human survival, have been extensively investigated. If improperly used, agricultural wastes, such as sawdust, rice husk, and straw, would likely harm human safety and health [1]. Hence, developing a novel and effective agricultural waste management system is a critical environmental challenge. In agricultural waste treatment, filter media are used as highly porous materials containing rough surfaces, which contribute to the creation of additional pores. This property improves microbial biofilm growth. Through calcination, sawdust can produce large pores in filter media [2,3]. This study aimed to develop a novel approach to solve problems related to agricultural wastes.

* Corresponding author.

Palygorskite, a naturally abundant clay mineral, is an excellent adsorbent employed in various conventional applications because of its large specific area [4]. The application of this clay mineral as an environmental adsorbent has been extensively investigated. It can naturally and efficiently adsorb colored components from vegetable oils and metal cations from cationic dyes and wastewater [5]. The adsorption capacity of palygorskite can be increased through chemical and/or thermal treatments without the loss of other physicochemical properties [6]. Xie et al. [7,8] reported that calcinated palygorskite was used as an adsorbent to remove phosphate from wastewater. Ye et al. [9] demonstrated that modified and natural palygorskite was used to remove phosphate ions from wastewater. Furthermore, modified and calcinated palygorskite can be used to remove phosphate efficiently.

Biological aerated filters (BAFs) are aerobic bioreactors that reduce energy consumption and maintain high organic load; these bioreactors have been widely used in advanced wastewater treatment [2]. Filter media are often used to load microbial biofilms; these media are necessary to treat wastewater during BAF operation. Dissolved oxygen (DO) concentration also affects the performance of BAF. DO in BAFs positively influences nitrification but negatively influences biological denitrification. DO can prevent denitrification because of its function as an electron acceptor from nitrate, and aerobic conditions inhibit denitrification-related enzymes [1,2]. A high DO concentration is also necessary to improve the activity of nitrifying bacteria in BAF; as a consequence, denitrification is repressed by DO. Denitrification is also suppressed by accumulated nitrite; thus, the quality of effluent from BAF decreases. Moreover, DO and nitrite are limiting factors of denitrification [1,2]. In China, commercially available ceramsite (CAC) has been commonly used as a filter medium in city wastewater treatment plants. However, CAC is composed of untreated clay as a raw material and exposed to high calcination temperatures (>1,200°C), which may destroy the crystal structure of clay [10,11]. As a result, CAC loses hydroxyl water; the microstructure of CAC collapses; and micropores are destroyed [12]. These events cause main problems related to BAFs; for instance, microbial biofilms are difficult to immobilize on CAC. The bioactivity and contaminant removal efficiencies of CAC-BAF are often low because the affinity of CAC to microbial biofilms is very poor as a result of poor surface biocompatibility and hydrophilicity [10,11]. Therefore, appropriate filter media that can serve as alternatives to CAC should be developed.

Novel filter media have been prepared for BAFs to enhance the latter's biodegradation capability [10,11]. For example, F. Sun and W.L. Sun [13] demonstrated the simultaneous removal of beryllium and ammonia nitrogen (NH_3–N) from smelting wastewater by using BAF. Zhang et al. [14] investigated the feasibility of an immobilized microbial biofilm containing anaerobic filters and BAFs as a novel material to treat 2,4,6-trinitrotoluene (TNT) red water. These filter media can efficiently remove nitrogen, beryllium, and TNT. However, the simultaneous removal of nitrogen and phosphorus (SNP) in BAF has been rarely reported [15].

Palygorskite porous ceramsite (PC) was developed in our previous research by using palygorskite clay mixed with sodium silicate and sawdust as filter media in BAF [6]. The present study aims to: (1) analyze the apparent properties of CAC and PC through scanning electron microscopy (SEM), porosimetry, thermogravimetry, X-ray fluorescence, and micro-computed tomography (micro-CT); (2) investigate the effects of air–water ratio (A/W) on the removal of total organic carbon (TOC), NH_3–N, total nitrogen (TN), and phosphorus in CAC and PC BAFs; and (3) evaluate the samples from CAC and PC BAFs. The filter media were covered with a growing microbial biomass collected from the top layer of the biofilter (1,500 mm), the middle layer of the biofilter (900 mm), and the bottom layer of the biofilter (300 mm). The present study also aims (4) to evaluate the characteristics of the microbial community in PC BAF through polymerase chain reaction (PCR)–denaturing gradient gel electrophoresis (PCR-DGGE).

2. Materials and methods

2.1. Materials

CAC, sawdust, sodium silicate, and palygorskite were obtained from Ma'anshan city, Hefei city, and Mingguang, Anhui Province, China.

2.2. Characterization and analytical methods

The multipoint Brunauer–Emmett–Teller surface area of PC and CAC was measured using a Quantachrome Nova 3000e automated surface area analyzer. X-ray fluorescence (XRF) chemical compositions of CAC and palygorskite were measured on a Shimadzu XRF-1800 with Rh target radiation. Elemental analysis (EA) of the sawdust was performed using a VARIO ELIII analyzer (Elemental Analysis System Co. Ltd., Germany). Surface morphologies were obtained with a Philips XL30 environmental scanning electron microscope at an accelerating voltage of 40 kV. The microscopic observation for the morphology of microbial biofilm was carried out using a U-RFL-T Olympus Biological Microscope (Japan). The growth of microbial biofilm biomass was determined according to the methods available in literature [6,16–18]. The thermal behavior of composite particles was measured in accordance with a previous study [19]. The physical characteristics of PC and CAC were measured in accordance with the sandstone pore structure method of image analysis [20]. The porosities of PC specimens were determined using micro-CT (μCT 40; Scanco Medical, Brüttisellen, Switzerland). The PC specimens were scanned in air at 70 kV and 57 μA, with an isotropic voxel size of 12 μm. A stack of 509 gray scale images was obtained, and a region of interest, which matches the exact circumference of the sample, was defined. A binary threshold was applied to each image, and Scanco built-in reconstruction algorithms were used to derive the porosity and to construct the 3-dimensional (3D) image [21–23]. The microbial populations in selected PC BAF were analyzed using domain-specific F341 R907 and PCR amplification of 16S rRNA gene fragments for genomic DNA from bacteria. The specific measures for the implementation were determined according to methods in literature [24,25].

2.3. Analysis of wastewater quality and characteristics

The wastewater samples were collected from the outlet and inlet pipes of CAC and PC BAFs. Chinese Environmental Protection Agency (EPA) standard methods were used to analyze TOC, NH_3–N, TN, and phosphorus [26]. Each experiment was divided into three stages. At each experimental test stage, the operating conditions of CAC BAF and PC BAF were recorded and summarized, as shown in Table 1. A stable hydraulic retention time of 7 h was used. The DO concentration was measured with a portable digital DO meter (Oxi-315, China).

2.4. Chemical composition of raw materials

The chemical compositions measured by EA indicated that the sawdust consisted of 46.09% C, 6.85% H, 35.09% O, 0.6% N, and 0.1% S, as well as small amounts of Cl, P, K, and Si. The majority of palygorskite clay consisted of SiO_2 (55.10%) and Al_2O_3 (9.60%), followed by Fe_2O_3 (5.70%) and MgO (10.70%). In addition to a few transition metal oxides (such as TiO_2, CaO, and MnO), a small amount of alkali-metal and alkaline-earth metal oxides that involve Na_2O and K_2O (1.01% in total) were present. SiO_2 and Al_2O_3 were the main components of ceramsite, and they constituted the glassy structure of ceramsite materials. The majority of CC consisted of SiO_2 (60.24%) and Al_2O_3 (17.94%), followed by Fe_2O_3 (13.16%) and minimal amounts of Cr_2O_3, MnO, CaO, MgO, K_2O, and Na_2O.

2.5. Preparation and sintering of PC

The preparation of PC includes the following steps (Figs. S1 and S2):

- The mixture of palygorskite clay, sodium silicate, and sawdust in the specified experimental mass ratio was placed in a small coating machine, which produced round granules with 7–13 mm diameter. The composite particles were dried at 110°C in the furnace.
- The composite particles were placed in a muffle furnace and heated at 700°C; afterward, the temperature was maintained for 3 h in an O_2 atmosphere.
- The calcinated composite particles were cooled to room temperature for 12 h. The synthesized composite particles were stored in a vacuum desiccator for future analysis.

3. Results and discussion

3.1. Differential thermal analysis (DTA) and thermogravimetric analysis

Fig. 1 shows the thermal analysis results of the composite particle (palygorskite/sodium silicate/sawdust). The DTA curve displays four endothermic valleys and three exothermic peaks. According to the crystal structure and chemical formula of palygorskite, four types of water exist: water

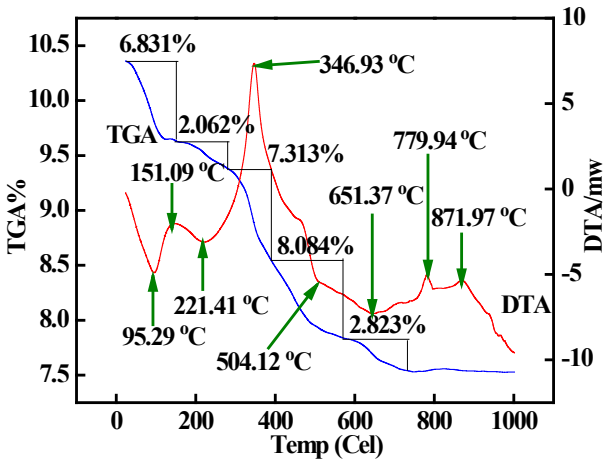

Fig. 1. Differential thermal analysis and thermogravimetric analysis patterns of composite particles.

Table 1
Operating conditions and average rate removals for PC and CAC in BAFs at different A/W

Sample	Operating conditions			Water quality indexes[a]		
	pH	T (°C)	A/W	TOC	NH_3–N	PO_4^{3-}
Stage one	6.7 (±0.5)	27°C–30°C	1:1	25.81–26.22	9.63–10.31	0.51–0.58
Stage two	6.6 (±0.5)	28°C–30°C	3:1	25.56–26.47	9.15–10.31	0.45–0.51
Stage three	7.1 (±0.5)	23°C–30°C	6:1	24.45–25.76	9.47–10.04	0.45–0.51
Average rate removals[b] for PC and CAC in BAF at different A/W						
A/W	1:1	3:1	6:1	1:1	3:1	6:1
Material						
	TOC (%)			NH_3–N (%)		
PC	18.07	52.87	74.40	17.64	76.10	86.15
CAC	16.70	35.06	50.77	15.33	52.27	79.81
	TN (%)			PO_4^{3-} (%)		
PC	17.44	45.70	28.57	72.33	77.71	75.49
CAC	8.09	15.64	14.95	34.21	33.97	32.55

[a]TOC, NH_3–N, and PO_4^{3-} values are given as influent concentrations in mg/L.
[b]All values are given as average removal rates in %.

adsorbed on the outer surface, water adsorbed in tunnels, water contained in the crystal structure, and structural water molecules coordinated with Mg(II) cations at the edge of octahedral sheets [8,27]. The first endothermic valley is found at 95.29°C. It represents the removal of the water adsorbed on the outer surface and in channels. This valley has a weight loss of 6.831%. The second endothermic valley is detected at 221.41°C. It represents the crystal water-absorbing effect produced by extrusion. This small and narrow endothermic valley exhibits 2.026% water loss. The third endothermic valley at 504.12°C is wide. It corresponds to the crystal degradation under thermal effects. This valley has 8.084% water loss. The fourth endothermic valley is located at 651.37°C. It corresponds to the degradation of the crystal structure. The amount of dehydration is 2.823%. The exothermic peaks detected at 779.94°C and 871.97°C are attributed to silicate hydrates, which are gradually dehydrated over a wide temperature range of up to 1,000°C [28]. The exothermic peak at 346.93°C indicates the release of CO_2 with 7.313% weight loss. This loss, which is caused by dehydration, is attributed to the decomposition of carbon materials: $C + O_2 \rightarrow CO_2$ [19]. The eutectic point of the composite particle can be reduced by the reaction of sodium silicate and CO_2 ($Na_2O{\cdot}nSiO_2{\cdot}xH_2O + CO_2 \rightarrow Na_2CO_3 + nSiO_2 + xH_2O\uparrow$) and by the dispersion of alkali metal oxide (such as Na_2O) originating from the decomposition of Na_2CO_3 ($Na_2CO_3 \rightarrow Na_2O + CO_2\uparrow$) in the heating process [28].

$$3\,(C_6H_{10}O_5) \rightarrow 8H_2O + C_6H_8O + 2CO\uparrow + 2CO_2\uparrow + CH_4\uparrow + H_2\uparrow + 7C \quad (1)$$

3.2. Micro-CT-based pore characterization of PC

The structural and porosity features of PC are analyzed and imaged with micro-CT. Micro-CT is used extensively to study porous materials, such as rocks or bones, and the applications of this technique in different areas are increasing [29–31]. Its popularity can be attributed to its ability to provide precise quantitative and qualitative information on the 3D morphology of porous materials. The interior of porous materials can be studied in great detail without resorting to physical sectioning [29–31]. Fig. 2(A) shows the 3D micro-CT reconstruction of PC. Fig. 2(A) also shows that PC has a rough surface, which is suitable for microbial biofilm growth. Sawdust, which is required to make the PC porous and rough, can produce tiny apertures inside the PC after being sintered [1,6]. Figs. 2(B)–(D) show the cross-sections of PC. These figures show that the pores are large, with diameters of approximately 500–1,000 μm (yellow arrows). The micro-CT analysis of PC shows a porosity of 25.25% with many unevenly distributed pores that is suitable for the growth of attached microorganisms. Porosity is an important factor to ensure successful simultaneous nitrification and denitrification (SND) in a given PC BAF process. The uneven distribution of DO and nutrient substances inside the pores of PC allows the simultaneous proliferation of nitrifying and denitrifying bacteria [1,6]. Thus, the structure of PC, including the dimension and morphology of the pores, is critical to allow nutrition and oxygen conduction

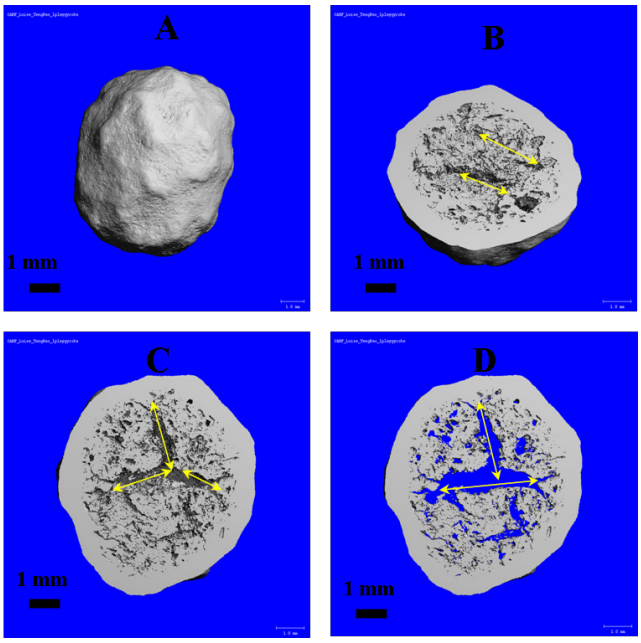

Fig. 2. Micro-CT of PC: (A) 3-dimensional reconstruction of PC; (B) horizontal cross-section of PC; (C) vertical cross-section of PC; and (D) 20 slices (0.72 mm) cross-section of PC.

and microbial biofilm growth into the pores. The microbial biofilm loaded into the pores of PC can maintain a high biofilm biomass concentration [1,6]. Micro-CT analysis shows that PC has spherical pores, which are interconnected with one another by window-like openings (Fig. 2). These interconnected spherical pores result in a large surface area; they also tend to result in a high biofilm biomass, thereby inducing high bioactivity [1,17].

3.3. Casting of thin sections of PC

BAFs, as a fixed microbial biofilm wastewater treatment process, generally promote an effective and SND process to remove nitrogen; this phenomenon is possible because the established oxygen gradient across the microbial biomass tends to induce SND that naturally occurs inside microbial biofilms [1,17]. Fig. 3 shows that the microbial biofilm loaded on the PC surface is a highly hydrophilic substance during the BAF operation [1,17]. Microbial biofilms can reach deep into the interior pores of PC (Figs. 3(A) and (B)), and microbial biofilms can be immobilized on the PC surface. Wastewater flow can be divided into three layers: aqueous adhesion layer, aerobic layer, and anoxic layer (Fig. 3(B)). Microbial biofilm contributes to the creation of these layers and favorite conditions for SND [1,17].

In a previous report, stained epoxy resin is used to impregnate the pore space of rock samples; this method effectively introduces pore spaces to rock samples. Although this method can be highly efficient in pore formation, few researchers use this method in porous filter media [32]. In this work, PC is prepared from palygorskite, sodium silicate, and sawdust. Stained epoxy resin is used to generate quantitative size and shape data from pores in the thin

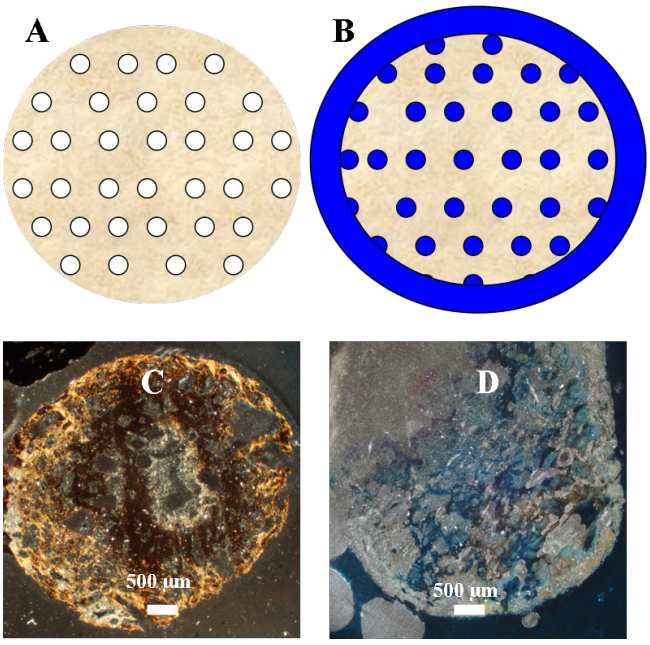

Fig. 3. Internal model and the porosity of PC: (A) models of the internal pores of PC; (B) filled of PC; (C) micrographs of PC after calcination (gray, PC); and (D) filled PC (dark blue, open pores).

section [32] and to obtain direct evidence supporting that microbial biofilm can be transferred via the PC structure. Fig. 3(C) reveals the intergranular pore textures in the thin section; the creamy white sections denote the molded PC, whereas the gray sections represent the intergranular pores of PC. This difference demonstrates that PC is characterized by a large volume of internal porosity accommodating guest microbial biofilm. The sizes of the interconnected pores and open pores are approximately 100–1,000 μm (Figs. 3(C) and (D)). The majority of bacteria are ≤0.5 μm in diameter; thus, the maximum amount of microbial biofilms can achieve sustained population growth in open pores. Impregnated with blue-dyed epoxy, the fully interconnected pores with 500 μm diameter can be determined from the white section. The results indicate that microbial biofilms can grow in the pores of PC and can participate for several processes. Microbial biofilm is first formed when some cells or bacteria are immobilized on the PC surface. After adhering to the substratum for some time, the cells or bacteria may consume nutrients and may begin to reproduce, grow, and produce extracellular polymers. Microbial biofilms rapidly develop in BAFs with adequate nutrients. Microbial biofilms can transform and degrade nitrogen, phosphorus, and organic compounds in wastewater. Furthermore, biofilms can be beneficial or detrimental depending on their location and biotransformation [17].

3.4. Comparison of the influence of A/W on TOC, TN, NH_4^+–N, and PO_4^{3-} removal using PC and CAC BAFs

In this work, the characteristics of BAFs with A/W of 1:1, 3:1, and 6:1 are determined. The influences of A/W on TOC and NH_4^+–N removal are shown in Fig. 4 and Table 1. A/W is closely related to the removal of TOC and NH_4^+–N when the A/W increases from 1:1 to 6:1. This increase favors the biodegradation in PC and CAC BAFs. In addition, a suitable DO concentration favors the growth of nitrifying bacteria to enhance nitrification. This trend is attributed to the increase in TOC and NH_4^+–N removal as the A/W increases from 1:1 to 6:1. In addition, a suitable A/W can effectively remove the aged biomass growing on the PC and CAC surfaces; consequently, the proliferation of denitrifying and nitrifying bacteria increases to achieve highly effective SND activity [33,34]. Nitrifying bacteria grow in the inner layer of the microbial biofilm. DO is mainly consumed by heterotrophic bacteria in the outer layer of the microbial biofilm with low A/W (1:1) that restricts the growth of nitrifying bacteria [33–35]. As the A/W increases, the increase in DO in the upper space of the reactor promotes the growth of nitrifying bacteria in the upper layer of BAF; as a result, NH_4^+–N accumulation decreases, and the NH_4^+–N removal rate increases. The concentrations of TOC and NH_4^+–N are higher in the effluent from PC BAF than in the effluent from CAC BAF. This difference can be attributed to the internal and surface pore structures of the PC. These structures are relatively well developed and uniform; consequently, the water-soluble organic substances, nutrients, and small suspended particles can reach deep in the pores of the PC. The available space for microbial biofilm growth, which is affected by the mass transfer rate of DO, and the dispersion of biofilm biomass are also improved by the extended ability of soluble pollutants to reach the pores in the PC; thus, the application of the filter layer increases the effectiveness of biofiltration [17].

The TN removal efficiencies initially improve but subsequently decrease as the DO concentrations increase (A/W), as shown in Fig. 4. The results imply that TN removal is remarkably affected by the DO concentrations in the two BAFs because oxygen respiration produces more energy than denitrification. As a consequence, a bacterial cell growing under aerobic conditions prefers to use oxygen as a terminal electron acceptor [36,37]. In addition to this competitive effect, oxygen controls denitrification in two levels: the regulation of gene expression and the reversible inhibition of denitrification enzyme activity [36,37]. The DO in the wastewater increases as the A/W is enhanced; thus, the degradation of organic substances is promoted by aerobic heterotrophic bacteria [36,37].

In PO_4^{3-} removal, the removal rates at different A/W values are listed and shown in Table 1 and Fig. 4; PC BAF displays a higher PO_4^{3-} removal than CAC BAF. In our previous reports, the highest phosphate removal capacity of palygorskite is achieved after calcination at 700°C. This trend is explained by the coordination of Al in palygorskite, which is transformed from six coordinates to four coordinates after calcination is completed. Moreover, the structure is transformed from crystalline to amorphous. The adsorbent yields the maximum adsorption capacity, and the coordination change in Al is closely related to the increased phosphate adsorption. Si–OH and Al–OH on the palygorskite surface are considered active sorption sites. The changes in Al coordination may alter the bond length and Al–O angle and may improve the binding activity between the Al–OH group and phosphate in wastewater [4,6–9]. Dolomite is present in palygorskite clay; naturally occurring dolomite ($CaMg(CO_3)_2$) is a double salt of calcium and magnesium carbonate. Dolomite

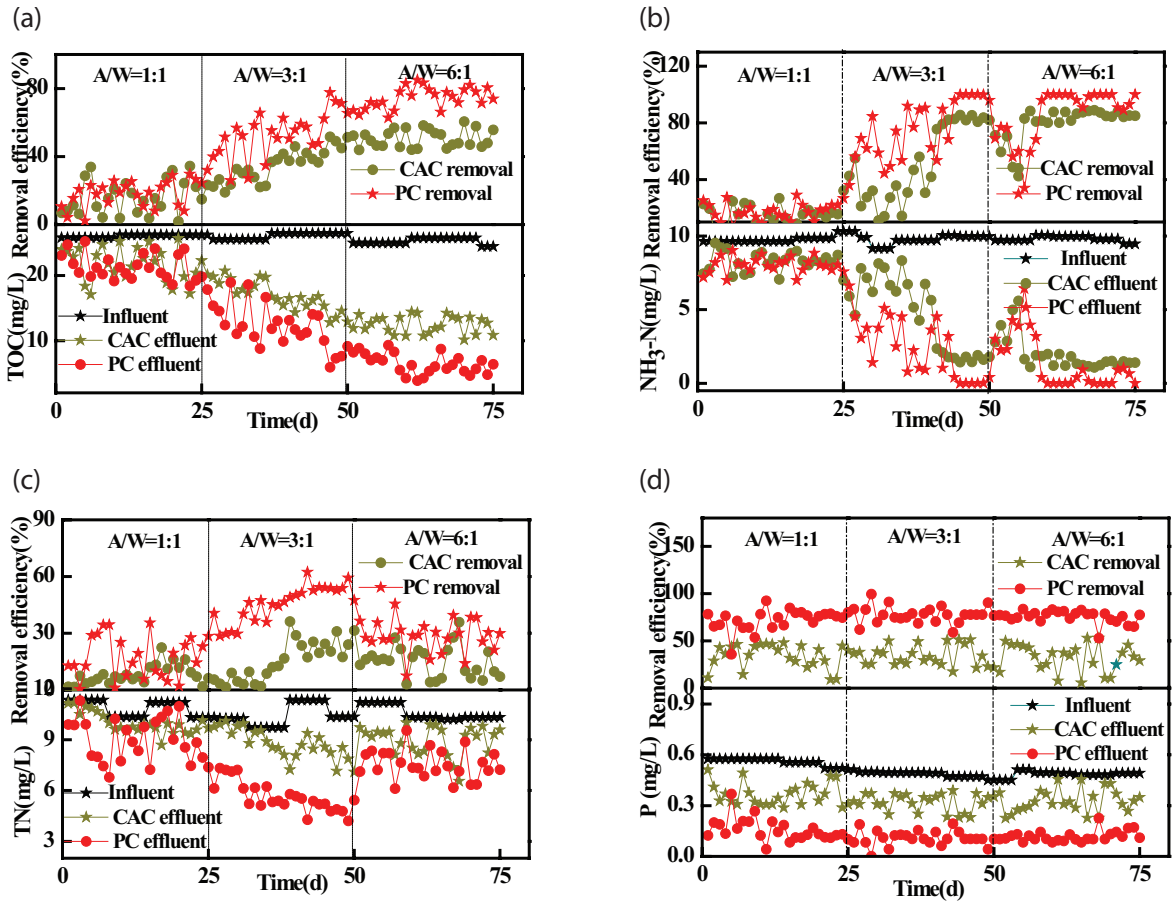

Fig. 4. Changes in the influent and effluent concentrations and removal efficiency of TOC, NH_3–N, TN, and PO_4^{3-} over time.

decomposes into CaO and MgO with increasing calcination temperature to 700°C. Therefore, phosphate should be adsorbed by Ca and Mg in natural and activated palygorskite [4,6–9]. As shown in the supplementary material (section 1.3), palygorskite is composed of Si, Mg, Al, and a small amount of Fe. CAC is mainly composed of 60.24% SiO_2 and 0.41% CaO. The CAC is high in SiO_2, but SiO_2 exhibits low PO_4^{3-} retention efficiency [38].

3.5. Microbial biofilm morphology by SEM

The surface morphologies of PC and CAC are observed with an SEM. Fig. 5(A) shows that the microbial biofilm is directly attached to the PC surface, and the microbial biofilm is apparently spread on the PC surface as indicated by the connections of extracellular secretions [17]. The microbial biofilm is relatively thick with aggregates. The good structure of the microbial biofilm can be maintained over time. The microstructure in Fig. 5(B) suggests that a large amount of microorganisms are immobilized on the outer and inner surfaces of the pores in the PC. PC is porous, and the size range, which facilitates the development of several microbial species, permits the efficient transfer of gas and liquids to the microorganisms via the pore canals. Figs. 5(C) and (D) show that the attached microbial biofilm is morphologically similar to the bacilli observed on the surface. Certain types of cocci can be observed to be the dominant microbes in the biomass (Figs. 5(E), (I), and (J)). In Fig. 5(H), the micrograph of PC clearly shows that some pores and coarse regions are irregularly distributed on the surface; these features are caused by the release of the accumulated gases that can be generated by the decomposition of sawdust matter in the composite particles during the sintering process [6,17]. Fig. 5(F) clearly shows that some pores with diameters of 6–10 μm are irregularly distributed on the smooth surface of the CAC. The microstructure in Fig. 5(G) suggests that a few microorganisms are immobilized onto the pore surfaces in CAC.

3.6. Two BAFs with different packing heights of biofilm biomass and microscopy of biofilm growth

The microbial biofilm morphology and biofilm biomass of two BAFs at different biological filler heights can be observed in Fig. 6 and summarized in Table 2. The biofilm biomass content quickly decreased when the media height was 0–1,500 cm in CAC-BAF and PC-BAF (Fig. 6(I)). The main reason for this trend is that the DO concentration at the bottom of the two BAFs was high and that the organic matter was abundant, thereby providing conducive conditions for the heterotrophic bacteria to grow in an optimum biomass concentration. Therefore, the biofilm thickness was high [33]. As shown in Figs. 6(II)(A) and (B), the microorganisms

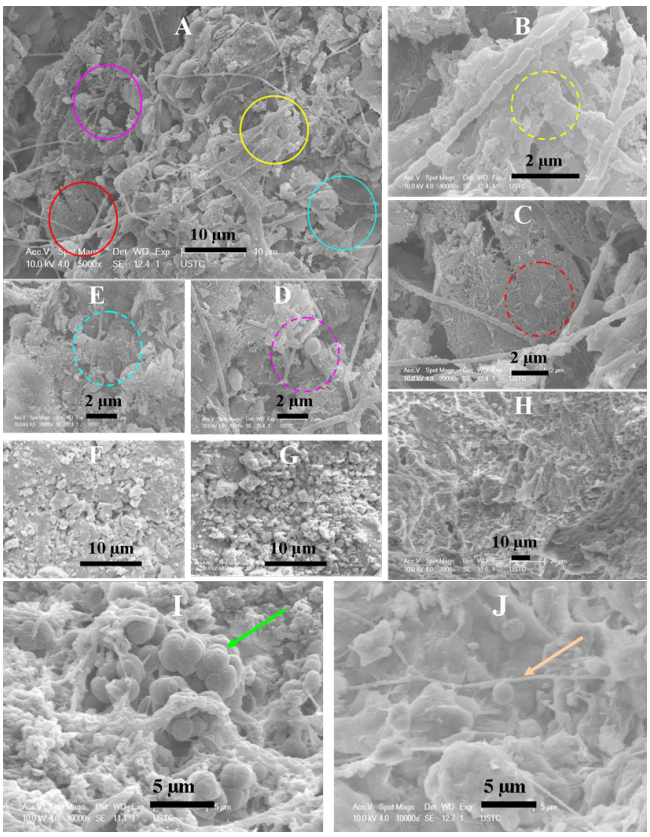

Fig. 5. SEM micrographs of the external surfaces of the PC and CAC after microbial loading. Microbial loaded on external surface of PC (A–E, I, J) and CAC (G). Raw external surface of (F) CAC and (H) PC.

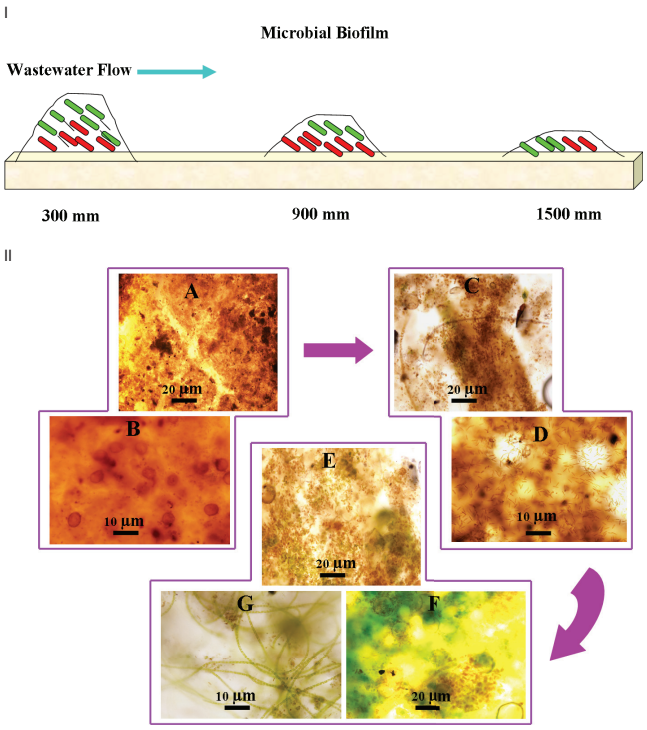

Fig. 6. PC BAF microbial biofilm morphology at different filler heights: (A) and (B) at the bottom (300 mm); (C) (D) in the middle (900 mm); and (E)–(G) on the top (1,500 mm).

Table 2
Microbial biofilm morphology and biofilm biomass in two BAFs at different biological filler heights

Microbial biofilm morphology			
Sample height (mm)	PC BAF Characteristics		
0–300	Deep brown; obvious fishy odor		
600–900	Light brown; no fishy odor		
900–1,500	Dust-colored; obvious aroma		
Biofilm biomass			
Media height, *h* (mm)	300	900	1,500
Material[a]			
PC	29.59	6.26	4.71
CAC	9.45	4.31	1.22

[a]Biofilm biomass values are given as concentrations in mg TN/g.

immobilized on PC in the BAFs included numerous globular microorganisms. Consequently, the biofilm biomass was greater at the 0–300 cm media height in the two BAFs. However, the DO concentration decreased with increasing media heights of the two BAFs, and the biomass concentration was also affected. Thus, the microbial biofilm became thinner, and the biofilm biomass lowered in the upper 300–900 cm of the filter media in the two BAFs. Numerous microorganisms continued growing in the system (Figs. 6(II) (C) and (D)). A large number of bacilli were immobilized on the surface of PC-BAF; these microorganisms may play a key role in the reduction of TN and other organic compounds in city wastewater. The biofilm biomass was lower in the upper 900–1,500 cm of the media in the two BAFs. Figs. 6(II) (E) and (F) show the abundance of microorganisms, such as *Cyanobacteria*, which are members of Cyanophyta. *Cyanophyta* is a phylum of bacteria that obtain energy through photosynthesis. The name "Cyanobacteria" originates from the color of the bacteria, which are often called blue–green algae [39].

3.7. Bacterial community analysis

PCR-DGGE is a well-known technology for biodiversity assessment in wastewater treatment [14]. In this study, PCR-DGGE is used to identify the bacterial community structure in PC BAF. The DGGE profiles of the amplified 16S rRNA fragments from the PC samples are shown in Fig. 7. Each of the distinguishable bands in the separation pattern represents an individual bacterial species [14]. Fig. 7 shows that certain bands (i.e., NO1, NO2, NO3, NO4, NO5, NO6, NO7, NO8, and NO9) are simultaneously found in Lanes 1, 2, and 3, thereby demonstrating the presence of several dominant bacterial groups for the treatment of city wastewater. The bands are excised from the gel, sequenced, and compared with those in the GenBank database to identify the dominant species in the bacterial community. The phylogenetic tree for the partial bacterial 16S rRNA sequences is presented in Fig. 8. Sequence NO2 is similar to *Flavobacterium* sp. 16S rRNA (JN679209.1). Sequence NO4 is similar to *Oscillatoriales*

cyanobacterium 16S rRNA (GQ324967.1). In addition, sequence NO5 is most closely related to *Sphaerotillus* sp. 16S rRNA (JQ945995.1). Sequence NO9 is similar to *Nitrospira* sp. 16S rRNA (LC055988.1). *Nitrospira* sp. can live in marine or nonmarine habitats. This genus is isolated from ocean water, freshwater, aquarium water, deltaic sediment, deep-sea sediments, soils, and an iron pipe of a heating system [40]. *Nitrospira* sp. is part of a nitrification process that is important in the biogeochemical nitrogen cycle; nitrification involves the oxidation of ammonia to nitrite by the autotrophic bacteria of the genus *Nitrosomonas* and the oxidation of nitrite to nitrate by the bacteria of the genus *Nitrospira* [40]. *Sphaerotilus natans* is an aquatic periphyton organism associated with polluted water. This species forms colonies that are commonly known as sewage fungus. These colonies are later identified as tightly sheathed filamentous bacteria. *S. natans* requires dissolved simple sugars or organic acids as its food supply, but it needs less phosphorus than the majority of other competing organisms; it can also tolerate low oxygen concentrations [41]. *O. cyanobacterium* belongs to the cyanobacterial genus *Limnothrix* Meffert, which is classified to the order Oscillatoriales of the family Pseudanabaenaceae and the subfamily Pseudanabaenoideae under the current botanical taxonomic system [39]. *Flavobacterium* sp. is found in soil and fresh water in various environments. This genus of gram-negative rod-shaped bacteria, which can be nonmotile or motile, consists of 130 recognized species. *Flavobacterium* sp. is capable of denitrification as a heterotroph or an autotroph; the genus includes facultative aerobic organisms with the ability to use oxygen as well as nitrate or nitrite; some species can also undergo fermentation in the absence of nitrate or oxygen [42–44].

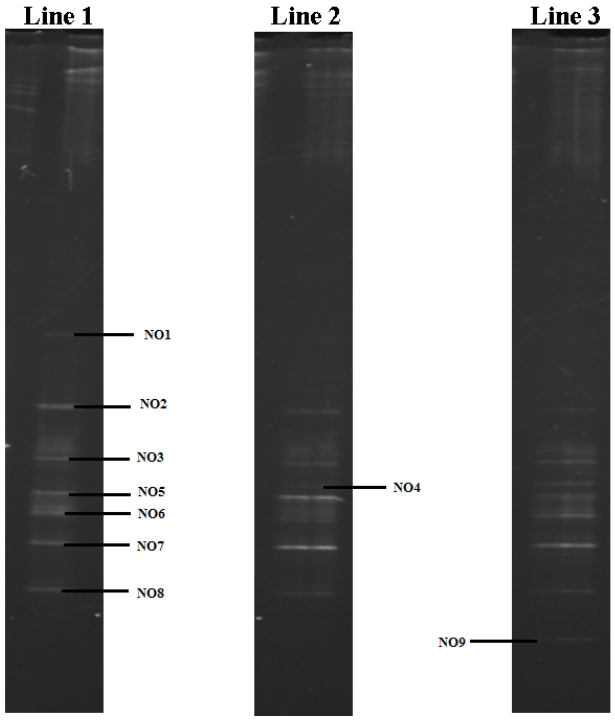

Fig. 7. DGGE profiles of bacteria and archaea 16S rRNA genes from the PC BAF.

4. Conclusions

- SEM, micro-CT, and porosimetry results suggest that the uniform and interconnected pores in PC are suitable for microbial growth. This conclusion is confirmed by the higher biofilm biomass obtained from the PC BAF than that from the CAC BAF after wastewater treatment is

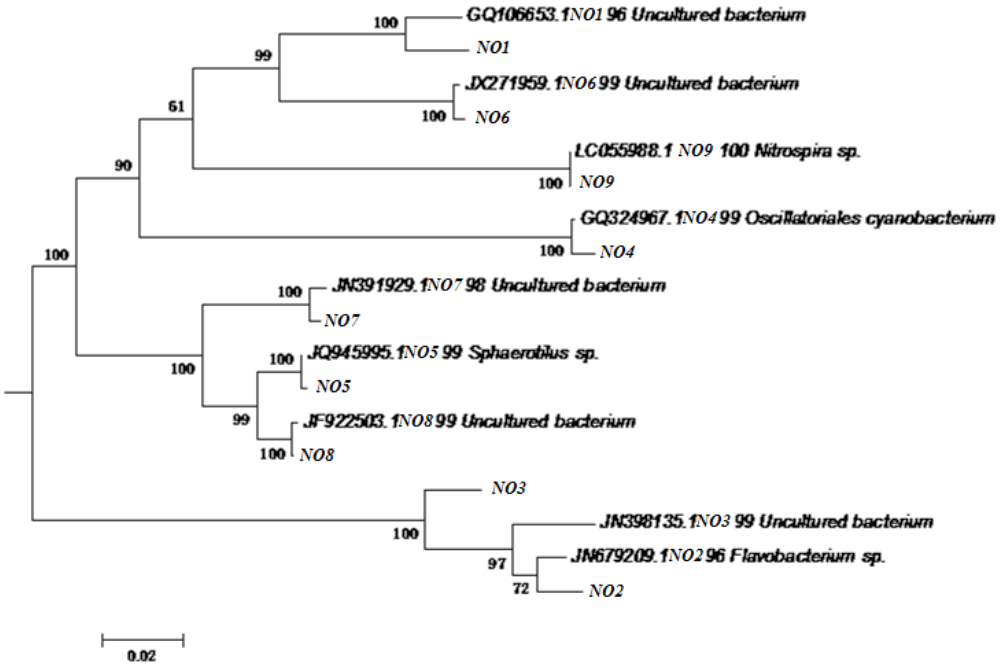

Fig. 8. Neighbor-joining tree showing the phylogenetic identity of the 16S rRNA of DGGE sequences obtained from DGGE bands.

completed under various A/W values of 1:1, 3:1, and 6:1. The results show that the efficiency of PC BAF is higher than that of CAC BAF in terms of TOC, TN, NH_3–N, and phosphorus removal. Therefore, PC is a novel and viable material to treat wastewater and to provide a promising use of sawdust waste material.

- The microbial biofilm pattern, color, and thickness of the BAFs gradually changed with wastewater flow. However, the microbial biofilm density was not evenly distributed vertically upward, and the portions near the PC surface exhibited a greater porosity than the other portions. The biofilm biomass decreased gradually with wastewater flow in the two BAFs. The composition of the microorganism population varied. The substances in the bottom layer were largely utilized. The dominant microbial population with different metabolism types may form along the wastewater flow. In addition, the optimum bacteria for the removal of city wastewater may be generated, as identified through PCR–DGGE. The combined species of nitrifying and denitrifying bacteria contribute significantly to the action of PC-BAF for city wastewater treatment.

Acknowledgment

We gratefully acknowledge the support by the National Natural Science Foundation of China (41072036, 41130206, 41372045, 41202021).

References

[1] K.L. Yang, Q.Y. Yue, W. Han, J.J. Kong, B.Y. Gao, P. Zhao, L. Duan, Effect of novel sludge and coal cinder ceramic media in combined anaerobic–aerobic bio-filter for tetracycline wastewater treatment at low temperature, Chem. Eng. J., 277 (2015) 130–139.
[2] W. Han, Q.Y. Yue, S.Q. Wu, Y.Q. Zhao, B.Y. Gao, Q. Li, Y. Wang, Application and advantages of novel clay ceramic particles (CCPs) in an up-flow anaerobic biofilter (UAF) for wastewater treatment, Bioresour. Technol., 137 (2013) 171–178.
[3] A. Bhatnagar, M. Sillanpaa, Utilization of agro-industrial and municipal waste materials as potential adsorbents for water treatment-a review, Chem. Eng. J., 157 (2010) 277–296.
[4] F.Q. Gan, J.M. Zhou, H.Y. Wang, C.W. Du, X.Q. Chen, Removal of phosphate from aqueous solution by thermally treated natural palygorskite, Water Res., 43 (2009) 2907–2915.
[5] G. Qiu, Q.Q. Xie, H.B. Liu, T.H. Chen, J.J. Xie, H.W. Li, Removal of Cu(II) from aqueous solutions using dolomite–palygorskite clay: performance and mechanisms, Appl. Clay Sci., 118 (2015) 107–115.
[6] T. Bao, T.H. Chen, C.S. Qing, J.J. Xie, R.L. Frost, Development and application of palygorskite porous ceramsite in a biological aerated filter (BAF), Desal. Wat. Treat., 57 (2016) 107–115.
[7] J.J. Xie, T.H. Chen, C.S. Qing, D. Chen, C.Z. Zhu, J.Y. Wang, X.M. Zhan, Adsorption of phosphate from aqueous solutions by thermally modified palygorskite, Environ. Eng. Manage. J., 12 (2013) 1393–1399.
[8] J.J. Xie, T.H. Chen, B.B. Xing, H.B. Liu, Q.Q. Xie, H.W. Li, Y.C. Wu, The thermochemical activity of dolomite occurred in dolomite–palygorskite, Appl. Clay Sci., 119 (2016) 42–48.
[9] H.P. Ye, F.Z. Chen, Y.Q. Sheng, G.Y. Sheng, J.M. Fu, Adsorption of phosphate from aqueous solution onto modified palygorskites, Sep. Purif. Technol., 50 (2006) 283–290.
[10] T. Bao, T.H. Chen, H.B. Liu, D. Chen, C.S. Qing, R.L. Frost, Preparation of magnetic porous ceramsite and its application in biological aerated filters, J. Water Process Eng., 150 (2014) 394–400.
[11] J. Werner, B. Besser, C. Brandes, S. Kroll, K. Rezwan, Production of ceramic membranes with different pore sizes for virus retention, J. Water Process Eng., 4 (2014) 201–211.
[12] W.F. Bradley, The structural scheme of attapulgite, Am. Mineral., 25 (1940) 405–410.
[13] F. Sun, W.L. Sun, Simultaneous removal of beryllium and ammonium–nitrogen from smelting wastewater in bench- and pilot-scale biological aerated filter, Chem. Eng. J., 210 (2012) 263–270.
[14] M.H. Zhang, G.H. Liu, K. Song, Z.Y. Wang, Q.L. Zhao, S.J. Li, Z.F. Ye, Biological treatment of 2,4,6-trinitrotoluene (TNT) red water by immobilized anaerobic–aerobic microbial filters, Chem. Eng. J., 259 (2015) 876–884.
[15] H.A.U. Hasan, S.R.S. Abdullah, S.K. Kamarudin, N.T. Kofli, Effective curves of completing simultaneous ammonium and manganese removal in polluted water using a biological aerated filter, J. Ind. Eng. Chem., 30 (2015) 153–159.
[16] Y.Z. Yu, Y. Feng, L.P. Qiu, W.W. Han, L.P. Guan, Effect of grain slag media for the treatment of wastewater in a biological aerated filter, Bioresour. Technol., 99 (2008) 4120–4123.
[17] J.L. Zou, G.R. Xu, K. Pan, W. Zhou, Y. Dai, X. Wang, D. Zhang, Y.C. Hu, M. Ma, Nitrogen removal and biofilm structure affected by COD/NH_4^+–N in a biofilter with porous sludge ceramsite, Sep. Purif. Technol., 94 (2012) 9–15.
[18] Y.F. Shen, Z.S. Zhang, Modern Biomonitoring Techniques Using Freshwater Microbiota, China Architecture & Building Press, Beijing, China, 1990 (in Chinese).
[19] T. Bao, T.H. Chen, M.L. Wille, X.H. Zou, R.L. Frost, C.S. Qing, D. Chen, Preparation of iron oxide-based porous ceramsite from goethite and its performance in biological aerated filters (BAFs), Desal. Wat. Treat., 57 (2016) 19216–19226.
[20] K. Ruzyla, D.L. Jezek, Staining method for recognition of pore space in thin and polished sections: research method paper, J. Sediment. Res., 57 (1987) 777–778.
[21] T. Hildebrand, P. Rüegsegger, A new method for the model-independent assessment of thickness in three-dimensional images, J. Microsc., 185 (1995) 67–75.
[22] T. Hildebrand, A. Laib, R. Mueller, J. Dequeker, P. Ruegsegger, Direct three-dimensional morphometric analysis of human cancellous bone: microstructural data from spine, femur, iliac crest, and calcaneus, J. Bone Miner. Res., 14 (1999) 1167–74.
[23] T. Hildebrand, P. Rüegsegger, Quantification of bone microarchitecture with the structure model index, Comput. Methods Biomech. Biomed. Eng., 1 (1997) 15–23.
[24] J. Tan, J. Wang, J. Xue, S.Y. Liu, S.C. Peng, D. Ma, T.H. Chen, Z.B. Yue, Methane production and microbial community analysis in the goethite facilitated anaerobic reactors using algal biomass, Fuel, 145 (2015) 196–201.
[25] X.Q. Zhao, L.Y. Yang, Z.Y. Yu, N.Y. Peng, L. Xiao, D.Q. Yin, B.Q. Qin, Characterization of depth-related microbial communities in lake sediment by denaturing gradient gel electrophoresis of amplified 16S rRNA fragments, J. Environ. Sci., 20 (2008) 224–230.
[26] Chinese EPA, Methods for Water and Wastewater Analysis, 4th ed., Environmental Science Publishing House of China, Beijing, China, 2002.
[27] T.H. Chen, J. Wang, C.S. Qing, S.C. Peng, Y.X. Song, Y. Guo, Effect of heat treatment on structure, morphology and surface properties of palygorskite, J. Chin. Chem. Soc., 34 (2006) 1406–1410.
[28] G.R. Xu, J.L. Zou, G.B. Li, Effect of sintering temperature on the characteristics of sludge ceramsite, J. Hazard. Mater., 150 (2008) 394–400.
[29] M. Ding, C.C. Danielsen, I. Hvid, S. Overgaard, Three-dimensional microarchitecture of adolescent cancellous bone, Bone, 51 (2012) 953–60.
[30] K. De, M. Boone, S. De, S. Van, H. Derluyn, B. Masschaele, A pore-scale study of fracture dynamics in rock using X-ray micro-CT under ambient freeze-thaw cycling, Environ. Sci. Technol., 49 (2015) 2867–2874.
[31] E. Cho, A. Sadr, N. Inai, J. Tagami, Evaluation of resin composite polymerization by three dimensional micro-CT imaging and nanoindentation, Dent. Mater., 27 (2011) 1070–1078.
[32] K. Ruzyla, D. Jezek, Staining method for recognition of pore space in thin and polished sections: research method paper, J. Sediment. Res., 57 (1987) 777–778.

[33] F. Liu, C.C. Zhao, D.F. Zhao, G.H. Liu, Tertiary treatment of textile wastewater with combined media biological aerated filter (CMBAF) at different hydraulic loadings and dissolved oxygen concentrations, J. Hazard. Mater., 160 (2008) 161–167.
[34] S.Q. Wu, Y.F. Qi, Q.Y. Yue, B.Y. Gao, Y. Gao, C.Z. Fan, S.B. He, Preparation of ceramic filler from reusing sewage sludge and application in biological aerated filter for soy protein secondary wastewater treatment, J. Hazard. Mater., 283 (2015) 608–616.
[35] B.J. Ni, H.Q. Yu, Y.J. Sun, Modeling simultaneous autotrophic and heterotrophic growth in aerobic granules, Water Res., 42 (2008) 1583–1594.
[36] J.M. Galvez, M.A. Gomez, E. Hontoria, L.J. González, Influence of hydraulic loading and air flow rate on urban wastewater nitrogen removal with a submerged fixed-film reactor, J. Hazard. Mater., 101 (2003) 219–229.
[37] M.A. Gomez, E. Hontoria, J.G. Lopez, Effect of dissolved oxygen concentration on nitrate removal from groundwater using a denitrifying submerged filter, J. Hazard. Mater., 90 (2002) 267–278.
[38] Y. Feng, Y.Z. Yu, L.P. Qiu, J.B. Wang, J.W. Zhang, The characteristics and effect of grain-slag media for the treatment of phosphorus in a biological aerated filter (BAF), Desal. Wat. Treat., 47 (2012) 258–265.
[39] M. Zhu, G. Yu, X. Li, W. Tan, R. Li, Taxonomic and phylogenetic evaluation of *Limnothrix* strains (Oscillatoriales, Cyanobacteria) by adding *Limnothrix planktonica* strains isolated from central China, Hydrobiologia, 698 (2012) 367–374.
[40] S. Ehrich, D. Behrens, E. Lebedeva, W. Ludwig, E. Bock, A new obligately chemolithoautotrophic, nitrite-oxidizing bacterium, *Nitrospira moscoviensis* sp. nov. and its phylogenetic relationship, Arch. Microbiol., 164 (1995) 16–23.
[41] P. Véronique, J. Stefan, W. Michael, C. Gilles, Morphological and biochemical properties of a *Sphaerotilus* sp. isolated from paper mill slimes, Appl. Environ. Microbiol., 65 (1999) 156–62.
[42] H.F. Zhuang, S.D. Shan, C.R. Fang, X.L. Yuan, Advanced treatment of biologically pretreated coal gasification wastewater using a novel expansive flow biological intermittent aerated filter process with a ceramic filler from reused coal fly ash, RSC Adv., 6 (2016) 39940–39946.
[43] E.J. Bateman, E.M. Baggs, Contributions of nitrification and denitrification to N_2O emissions from soils at different water-filled pore space, Biol. Fertil. Soils, 41 (2005) 379–388.
[44] J.P. Carter, Y.H. Hsaio, S. Spiro, D.J. Richardson, Soil and sediment capable of aerobic nitrate respiration, Appl. Environ. Microbiol., 61 (1995) 2852–2858.

Supplementary material

1. Reactor description

Two laboratory-scale biofilter columns were constructed from polyvinylchloride pipes, as shown in Fig. S3, The pipes were 6 cm in diameter with a depth capable of approximately 150 cm of commercially available ceramsite (CAC) and porous ceramsite (PC). Of the two biological aerated filters (BAFs), one was packed with PC, and the other was composed of CAC. Horizontal sampling ports were installed at three depths (300, 900, and 1500 mm from the upper surface of the carriers) to allow the collection of samples for water quality analysis.

Acknowledgment

We gratefully acknowledge the support by the National Natural Science Foundation of China (41072036, 41130206, 41372045, 41202021).

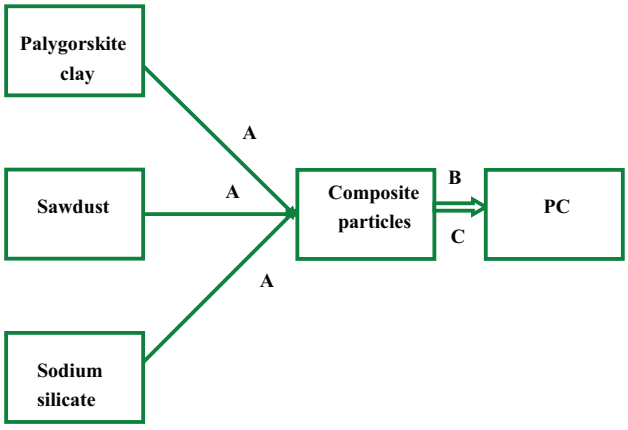

Fig. S1. Schematic of PC preparation: (A) drying, pulverizing, sieving, mixing, and pelleting; (B) sintering at 700°C 180 min; and (C) cooling down.

Fig. S2. Comparison of CAC and PC. Micrographs of: (A) CAC and (B) PC.

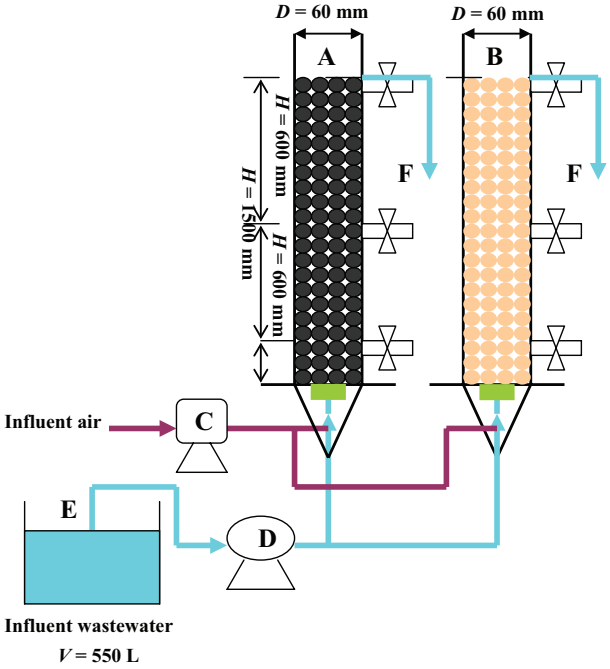

Fig. S3. Schematic of the BAF system: (A) CAC BAF; (B) PC BAF; (C) air blower; (D) water pump; (E) wastewater tank; and (F) effluent pipe.

Table S1
Regulatory levels of ceramics in PC and CAC

Item	PC experimental levels	CAC experimental levels
Grain diameter, d (mm)	5–8	4–6
Silt carrying capacity, C_s (%)	0.27	≤1
Solubility in hydrochloric acid, C_{ha} (%)	0.434	≤1.5
Void fraction, υ (%)	69	>42
Specific surface area, S_w (cm²/g)	6.1×10^5	$\geq 2 \times 10^4$
Piled density, ρ_p (g/cm³)	0.53	≤1.0
Apparent density, ρ_{ap} (g/cm³)	1.71	1.4–1.8
Compression strength, N	50–58	≥87
Porosity, P (%)	25.25	3.46